

Use of Completely Mixed Flow-Through Systems: Hydrolysis of Phenyl Picolinate

MICHAEL GFELLER,*
GERHARD FURRER, AND
RAINER SCHULIN

Institute of Terrestrial Ecology, Swiss Federal Institute of Technology (ETHZ), Grabenstrasse 3, CH-8952 Schlieren, Switzerland

Experimental equipment was developed to study the hydrolysis of environmentally relevant compounds in completely mixed flow-through reactors. The hydrolysis of a carboxylic acid ester, phenyl picolinate (PhP), was investigated in homogeneous solutions and in the presence of titanium dioxide particles. In the absence of solids, the hydrolysis of PhP is dominated by the acid-catalyzed reaction below pH 4 and by the base-catalyzed reaction above pH 5, while the neutral hydrolysis is of minor importance across the whole pH range investigated ($2 < \text{pH} < 8$). However, in presence of $10 \text{ g of TiO}_2 \text{ L}^{-1}$ ($\approx 420 \text{ m}^2 \text{ surface area L}^{-1}$), the neutral, surface-catalyzed reaction dominated the overall hydrolysis process in the entire range from pH 2 to pH 9. Steady-state rates of the heterogeneous hydrolysis were about 1 order of magnitude slower in completely mixed flow-through systems than initial hydrolysis rates in batch systems. This was attributed to reaction products occupying reactive sites at the mineral surface, thus hindering the adsorption of the educt PhP.

1. Introduction

Many widely used pesticides are carboxylic acid esters, phosphoric acid esters, and carbamates. Under certain pH conditions, they readily hydrolyze in water. Among other transformation reactions, hydrolysis is important for the mineralization of pesticide compounds in the environment. Dissolved metal ions and mineral surfaces are known to increase hydrolysis rates of organic esters (1, 2). Dissolved metal ions or surface metal centers may catalyze this reaction by direct polarization of chemical bonds in the organic compound. In both cases, the water molecule with its dipole character may be sufficiently nucleophilic to induce the hydrolysis reaction. If the organic ester and the metal ion form bidentate complexes, polarization may be enhanced as compared to the monodentate complex. Fife and Przystas (3) have investigated the influence of divalent metals (Ni^{2+} and Cu^{2+}) on the hydrolysis rate of picolinate esters. They have found substantial rate enhancement if the pyridine nitrogen is in ortho position to the ester function, leading to the formation of a chelate with the dissolved metal ion. A surface-catalytic effect on the hydrolysis of the ester phenyl picolinate (PhP; Figure 1) has been reported by Torrents and Stone (4) in a heterogeneous systems containing TiO_2 or goethite (FeOOH). In other words, metal ion and surface catalysis may lead to an increase in reaction rates in a broad pH range, depending on the speciation of the chelate. The

influence of such chelate-induced catalysis may be most pronounced in the pH range where the half-life in homogeneous solutions is longest. In most environmental systems, however, the concentration of free metal ions is probably too low to play an important role in degradation of organic compounds (1, 5). Mineral surfaces, however, are present in such abundance that they may exert a significant catalytic effect.

Hydrolysis reactions of organic compounds relevant in the environment have usually been studied in batch reactors measuring initial rates. Advantages of batch methods are that they generally require only low-cost equipment and are easy to use. They are of limited use for the investigation of long-term effects that become manifest in the time span exceeding the instant reaction phenomena observed at the beginning of an experiment. One possible long-term effect is the inhibition of a surface-catalytic process due to adsorption of reaction products on the reactive sites of the mineral. This effect may be difficult to observe in batch reactors, unless reaction products are added at the beginning of an experiment or the reaction solution is repeatedly spiked with the reaction educt. The determination of initial rates from batch experiments is often difficult, particularly if the reaction mechanism is complex or changes with time.

We have therefore developed an alternative method for the investigation of hydrolytic degradation of pesticides in model soil systems. The experimental setup is based on the completely mixed flow-through reactors described by Furrer et al. (6). For convenience, we subsequently replace the term "completely mixed flow-through reactor" by "mixed flow reactor" as it is used in chemical engineering (7). If the material fluxes across the boundaries of this type of reactor remain constant, steady state may eventually be reached. Steady-state data can be analyzed using the computer program SteadyFit, which allows the simultaneous determination of kinetic and thermodynamic constants (8). One of the advantages of using mixed flow reactors is that reaction rates can be determined directly from the concentrations of the reactants in the outflow. Furthermore, inhibition by co-adsorbed species can be more easily observed in mixed flow reactors than in batch reactors (9).

The setup has been tested by re-analyzing the surface-catalyzed hydrolysis of the carboxylic acid ester phenyl picolinate (PhP) in the presence of TiO_2 , which has been extensively studied in batch systems by Torrents and Stone (4, 10, 11). The hydrolysis of PhP occurs via homogeneous as well as heterogeneous parallel reactions as shown in Figure 1. Hydrolysis products are picolinic acid and phenol. Figure 2 shows the structures of all organic compounds used in the experiments, including protonated and deprotonated species. Experiments have been performed in homogeneous systems for a direct comparison of hydrolysis rates with literature data. Heterogeneous experiments have been conducted to study the differences between initial reaction rates obtained from batch experiments and steady-state rates obtained using mixed flow reactors.

2. Materials and Methods

Phenyl picolinate was synthesized according to Bald (12). TiO_2 (type P25) was provided by Degussa Corp. and used without further treatment. It consisted of about 40% rutile and 60% anatase (R. Giovanoli, 1992, personal communication). All solutions and suspensions were prepared with purified water with a resistivity of $18 \text{ M}\Omega \text{ cm}$ (Barnstead NANOpure). Argon (99.998%) was obtained from PanGas. All other chemicals were of analytical grade or better and were obtained from either Merck or Fluka. All experiments

* Corresponding author phone: +41 1 633 60 13; fax: +41 1 633 11 23; e-mail: gfelder@ito.umnw.ethz.ch.

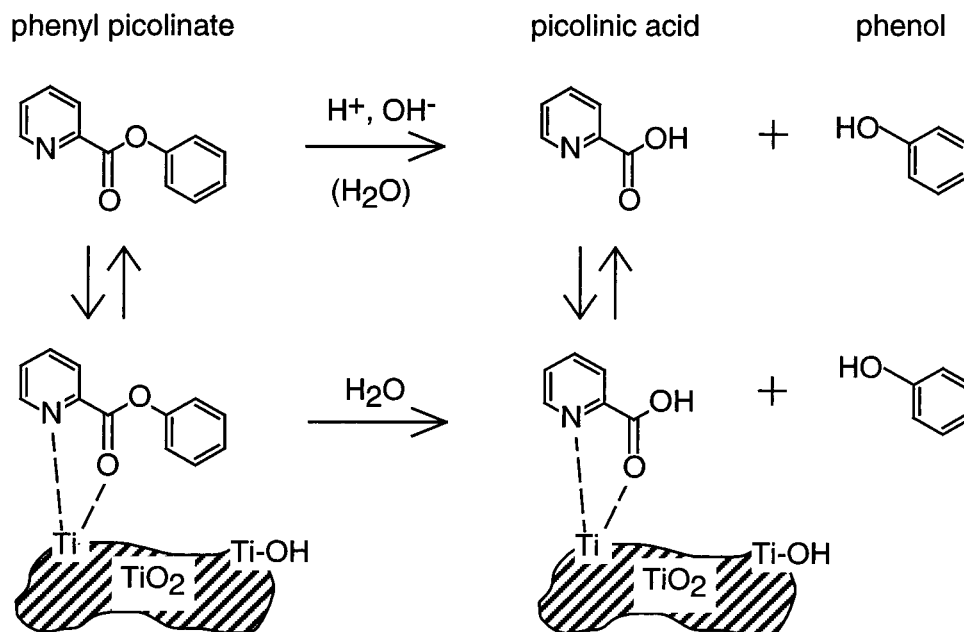


FIGURE 1. Reaction scheme of the hydrolysis of phenyl picolinate in heterogeneous system with TiO_2 . No protonation equilibria are shown. While in the homogeneous solution, the hydrolysis reaction occurs predominantly as H^+ or OH^- catalyzed (the neutral reaction is much less important); the surface-catalyzed reaction is not pH dependent in the investigated pH range.

were performed at 25°C and an ionic strength of 0.1 (adjusted with NaCl). For the experiments with TiO_2 , reaction solutions were protected against light by black plastic foil to prevent photochemical reactions. The pH electrodes were calibrated by performing acid–base titrations in the absence of particles to obtain values for the parameters E_0 and k of the Nernst equation $E = E_0 + k \log [\text{H}^+]$. From the measured emf values E , the pH values were calculated according to $\text{pH} = (E_0 - E)/k$.

2.1. Batch Experiments. Batch systems were used for acid–base titrations of TiO_2 and to determine adsorption curves for picolinic acid, phenol, and 2-benzoylpyridine on TiO_2 .

Titration of TiO_2 . For each titration, 10 mL of a 0.2 M NaCl solution was added to 10 mL of a ca. 25 g L^{-1} TiO_2 suspension in a thermostated beaker. The suspension was purged with Ar and stirred with a hanging Teflon propeller. Acid (0.01 M HCl) or base (0.01 M NaOH) were added using a computer-controlled dosimat (Metrohm 665). After each addition, the concentration of the free hydrogen ions was determined by emf measurements using a combined microglass electrode (Metrohm 6.0204.100) and a computer-controlled pH meter (Metrohm 713). Equilibrium was assumed when the standard deviation of 10 subsequent measurements, taken every 60 s, was less than 0.3 mV. The average value of these 10 measurements was used for further evaluation. If the number of measurements exceeded 30 without the stability criteria being met, the data point was discarded. Separate batches were used for the titration of TiO_2 with acid and base, with an initial concentration of 11.217 and 12.083 g L^{-1} TiO_2 , respectively.

Adsorption Curves. Adsorption curves for picolinic acid (1.0×10^{-4} M), phenol (1.022×10^{-5} M), and 2-benzoylpyridine (1.5×10^{-4} M) were determined separately in suspensions containing 10.100, 10.583, and 9.967 g L^{-1} TiO_2 , respectively. For each pH, separate flasks were used. The initial pH was adjusted by adding either 0.1 M HCl or 0.1 M NaOH. After purging with Ar for 1 h, the suspensions were equilibrated during 24 h at 130 rpm on a shaker. The pH was measured before analysis. Samples containing picolinic acid or phenol were filtered through a 0.01- μm cellulose–nitrate filter (Sartorius). Picolinic acid was analyzed at pH = 1 (glycine–hydrochloride buffer) at 270 nm using a spectrophotometer

(UVIKON 930, Kontron). Phenol was determined by reversed phase HPLC (see below). Solutions containing 2-benzoylpyridine were centrifuged at 20000 rpm (70000g) for 2 h (Centrikon T-1170, rotor TST 28.28/17). The supernatant was analyzed like the picolinic acid filtrate. Adsorption experiments with 2-benzoylpyridine were conducted in duplicates, phenol concentrations were measured after 1, 2, and 3 days. The acid–base titrations and the adsorption experiments were evaluated with the computer program GRFIT (13), applying the constant capacitance surface complexation model (14).

2.2. Mixed Flow Experiments. The reactors used have been described by Furrer et al. (6). We used between four and eight reactors concurrently. The experimental setup is described in detail elsewhere (15). The pH was adjusted using either HCl or NaOH. Phenyl picolinate and phenol were analyzed by reversed phase HPLC (two pumps: JASCO PU-980, UV-detector: JASCO UV-970, wavelength: 270 nm, degasser: GAS TORR GT-130, column: LiChrospher 100 RP-18 (Merck 50943.0001), eluent: 60% methanol and 40% acetic acid–sodium acetate buffer (5 mM each), flow: 1 mL min^{-1}). HPLC peak areas were integrated using a chromatographic data system (JCL6000, Jones Chromatography, U.K.). The factors for the conversion of peak areas to concentrations were determined by calibrations before and after an experiment and used to obtain the conversion factors at time t by linear interpolation.

Daily, the flow velocity of the reaction solution was determined gravimetrically. The residence time (τ) was calculated by dividing the reactor volume (ca. 60 mL), which was determined gravimetrically after each experiment, by the average flow rate of an experiment. The steady-state pH for experimental series 1–5 (see Tables 1 and 2) was determined by collecting about 10 mL of outflow solution and subsequent measurement, usually several times during an experiment. In series 6 and 7, the pH was determined on-line as described by Furrer et al. (15). The electrodes were calibrated as described above before and after the experiments. The pH values were calculated from the emf measurements by linear interpolation of the parameters E_0 and k of the Nernst equation.

2.3. Treatment of Data from Mixed Flow Experiments. In the following discussion, the average of variable c (e.g., concentration) from data point n_0 to n_1 is denoted by $\bar{c}_{n_0}^{n_1}$ and

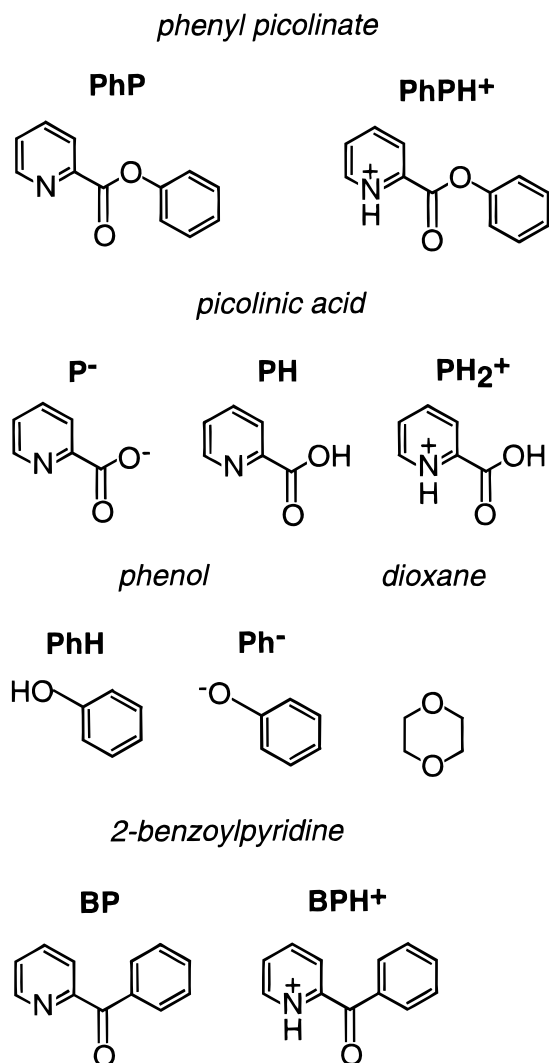


FIGURE 2. Structures and abbreviations of all organic species. Dioxane was used as cosolvent.

its standard deviation by $\bar{c}_{n_p}^m$. The term “data point” refers to a pair of concentrations of phenyl picolinate (PhP) and phenol (PhH). In this section, the notations [PhP] and [PhH] refer to the total dissolved concentration of these compounds.

Removal of Outliers. A data point u ($u > 1$) was removed before the determination of the steady state if at least one of the conditions

$$|[\text{PhP}]_u - \overline{[\text{PhP}]_{u-1}^{u+1}}| > fa_{\text{PhP}} \quad (1)$$

or

$$|[\text{PhH}]_u - \overline{[\text{PhH}]_{u-1}^{u+1}}| > fa_{\text{PhH}} \quad (2)$$

was fulfilled, where a_{PhP} and a_{PhH} denote the maximal absolute error allowed for PhP and PhH, respectively. The constant f was set to 3. This simple algorithm sometimes caused the removal of data in the transient state. However, this was never crucial for the steady-state determination.

Determination of Steady State. The optimization of the rate constants using SteadyFit (8) requires the determination of the steady-state concentrations of phenyl picolinate ($[\text{PhP}]_{\text{sts}}$) and phenol ($[\text{PhH}]_{\text{sts}}$) and of the measurement errors σ_{PhP} and σ_{PhH} . The determination of steady-state values was performed with the reduced data set, i.e., after outliers were removed.

TABLE 1. Experimental Conditions and SteadyFit Input Data for the Homogeneous System^a

id	v	$[\text{H}^+]_{\text{in}}$	$[\text{PhP}]_{\text{in}}$	$[\text{H}_2\text{CO}_3]_{\text{in}}$
1.5	6.78E-06	9.87E-04	6.72E-05	1.88E-08
2.4	1.32E-05	9.92E-05	6.15E-05	1.90E-08
2.5	1.29E-05	9.91E-03	6.29E-05	1.89E-08
3.4	1.39E-05	2.98E-03	8.26E-05	1.89E-08
3.5	1.38E-05	2.98E-04	8.32E-05	1.89E-08
3.6	1.39E-05	2.98E-05	8.14E-05	1.94E-08
5.5	1.38E-05	1.00E-07	8.34E-05	9.75E-08
5.6	1.36E-05	-9.92E-07	8.36E-05	4.83E-07
5.7	1.35E-05	-9.92E-06	8.48E-05	4.54E-06
5.8	1.36E-05	-9.92E-05	8.25E-05	4.60E-05
6.3	1.50E-05	-9.93E-06	7.67E-05	4.54E-06
6.4	1.37E-05	-9.92E-07	8.32E-05	4.83E-07
7.5	1.44E-05	9.92E-03	8.24E-05	1.89E-08
7.8	1.38E-05	-4.96E-05	8.32E-05	2.28E-05

id	$[\text{PhP}]_{\text{sts}}$	σ_{PhP}	$[\text{PhH}]_{\text{sts}}$	σ_{PhH}
1.5	3.80E-05	1.88E-06	2.64E-05	1.53E-06
2.4	5.76E-05	1.50E-06	4.60E-06	7.71E-07
2.5	2.65E-05	1.06E-06	3.53E-05	7.35E-07
3.4	5.38E-05	2.00E-06	2.66E-05	1.58E-06
3.5	7.69E-05	1.99E-06	4.23E-06	1.76E-06
3.6	7.46E-05	1.92E-06	4.44E-06	1.57E-06
5.5	7.43E-05	1.66E-06	1.07E-05	1.14E-06
5.6	7.76E-05	1.29E-06	5.58E-06	5.43E-07
5.7	6.89E-05	9.89E-07	1.57E-05	5.67E-07
5.8	2.95E-05	1.18E-06	5.15E-05	1.60E-06
6.3	7.46E-05	7.39E-07	3.16E-06	7.67E-07
6.4	8.01E-05	1.62E-06	4.83E-06	1.42E-06
7.5	3.64E-05	1.42E-06	4.51E-05	1.67E-06
7.8	6.56E-05	1.63E-06	1.87E-05	1.19E-06

^a id, experiment identification (series number before the period, experiment number within a series after the period); v , volume-normalized flow (s^{-1}); $[\text{H}^+]_{\text{in}}$, concentration of H^+ in the inflow; $[\text{PhP}]_{\text{in}}$, concentration of PhP in the inflow; $[\text{H}_2\text{CO}_3]_{\text{in}}$, concentration of H_2CO_3 in the inflow; $[\text{PhP}]_{\text{sts}} \pm \sigma_{\text{PhP}}$ and $[\text{PhH}]_{\text{sts}} \pm \sigma_{\text{PhH}}$, steady-state concentration of PhP and PhH (with error). All concentrations are in mol L^{-1} .

The absolute errors of PhP (α_{PhP}) and PhH (α_{PhH}) were set equal to the standard deviations of [PhP] and [PhH] in the steady-state range from data points n_0 to n_1 :

$$\alpha_{\text{PhP}} = \overline{[\text{PhP}]_{n_0}^{n_1}} \quad (3)$$

$$\alpha_{\text{PhH}} = \overline{[\text{PhH}]_{n_0}^{n_1}} \quad (4)$$

The absolute errors were used as a first criterion to determine steady state because the spread about the average concentrations is large if (1) concentrations steadily increase or decrease (i.e., the rate of change is large) and (2) measurements deviate from a horizontal course of concentrations. Since the absolute error for PhP and PhH must be simultaneously small, it was required that

$$\alpha_{\text{PhP}} \leq a_{\text{PhP}} \quad (5)$$

$$\alpha_{\text{PhH}} \leq a_{\text{PhH}} \quad (6)$$

were both true. The maximum absolute errors allowed for PhP and PhH, a_{PhP} and a_{PhH} , were both set to 10^{-6} M.

Because the mass balance must be sufficiently close to 100% at steady state, a further criterion could be applied. Assuming that phenyl picolinate and phenol are consumed and produced solely by hydrolysis, the sum of their concentrations at steady state should be equal to the concentration of phenyl picolinate in the inflow, $[\text{PhP}]_{\text{in}}$:

$$[\text{PhP}]_{\text{in}} = [\text{PhP}]_{\text{sts}} + [\text{PhH}]_{\text{sts}} \quad (7)$$

TABLE 2. Experimental Conditions and SteadyFit Input Data for the Heterogeneous System^a

id	[TiO ₂]	<i>v</i>	[H ⁺] _{in}	[PhP] _{in}	[H ₂ CO ₃] _{in}
1.1	9.31	6.69E-06	9.87E-03	6.71E-05	2.91E-08
2.1	9.27	1.27E-05	9.91E-05	6.21E-05	2.95E-08
2.2	9.38	1.29E-05	9.92E-03	6.16E-05	2.93E-08
2.3	9.58	1.28E-05	9.91E-04	6.38E-05	2.93E-08
3.1	12.69	1.44E-05	2.98E-03	7.87E-05	2.93E-08
3.2	12.79	1.52E-05	2.98E-04	7.51E-05	2.94E-08
3.3	13.12	1.41E-05	2.98E-05	8.30E-05	3.00E-08
5.1	7.30	1.36E-05	1.00E-07	8.30E-05	1.38E-07
5.3	7.52	1.35E-05	-9.92E-06	8.56E-05	5.59E-06
5.4	7.40	1.40E-05	-9.92E-05	8.16E-05	5.45E-05
7.4	9.90	1.35E-05	-4.96E-05	8.76E-05	2.75E-05

id	[PhP] _{sts}	σ _{PhP}	[PhH] _{sts}	σ _{PhH}
1.1	1.76E-05	6.28E-07	4.96E-05	1.15E-06
2.1	3.60E-05	1.29E-06	2.68E-05	1.33E-06
2.2	2.37E-05	1.14E-06	3.67E-05	1.50E-06
2.3	3.59E-05	1.28E-06	2.71E-05	1.31E-06
3.1	4.36E-05	1.74E-06	3.35E-05	1.60E-06
3.2	5.26E-05	1.27E-06	2.19E-05	1.24E-06
3.3	5.26E-05	2.14E-06	2.75E-05	2.13E-06
5.1	5.03E-05	8.03E-07	3.19E-05	8.05E-07
5.3	5.93E-05	1.24E-06	2.53E-05	6.61E-07
5.4	3.57E-05	1.17E-06	4.52E-05	1.18E-06
7.4	4.82E-05	2.67E-06	3.58E-05	2.24E-06

^aid, experiment identification (series number before the period, experiment number within a series after the period); [TiO₂], concentration of TiO₂ (g L⁻¹); *v*, volume-normalized flow (s⁻¹); [H⁺]_{in}, concentration of H⁺ in the inflow; [PhP]_{in}, concentration of PhP in the inflow; [H₂CO₃]_{in}, concentration of H₂CO₃ in the inflow; [PhP]_{sts}, ± σ_{PhP} and [PhH]_{sts}, ± σ_{PhH}, steady-state concentration of PhP and PhH (with error). All concentrations are in mol L⁻¹.

We thus defined the relative error for data point *u* in the mass balance as

$$\mu_u = \frac{[\text{PhP}]_{\text{in}} - ([\text{PhP}]_u + [\text{PhH}]_u)}{[\text{PhP}]_{\text{in}}} \quad (8)$$

Instead of requiring that μ was smaller than a fixed number (*m*), we imposed the condition that the relative errors of both PhP and PhH were smaller than a value derived from *m*, which was set to 0.05.

The relative error of PhP was defined as

$$\rho_{\text{PhP},u} = \left| \frac{[\text{PhP}]_u - [\text{PhP}]_u^*}{[\text{PhP}]_u^*} \right| \quad (9)$$

where [PhP]_u^{*} is the mean of the measured PhP concentration ([PhP]_u) and the concentration calculated from the measured phenol concentration ([PhP]_{in} - [PhH]_u):

$$[\text{PhP}]_u^* = \frac{[\text{PhP}]_u + ([\text{PhP}]_{\text{in}} - [\text{PhH}]_u)}{2} \quad (10)$$

By combining eqs 8–10, the relative error of PhP, ρ_{PhP,u}, can be linked to the relative mass balance error, μ_u:

$$\rho_{\text{PhP},u} = \left| \frac{-[\text{PhP}]_{\text{in}} \mu_u}{2[\text{PhP}]_u^*} \right| \quad (11)$$

Substitution of μ_u by *m*, the maximal allowed relative error for the mass balance, in eq 11 yields the maximal allowed relative error for PhP, *r*_{PhP,u}:

$$r_{\text{PhP},u} = \left| \frac{-[\text{PhP}]_{\text{in}} m}{2[\text{PhP}]_u^*} \right| \quad (12)$$

This leads to the second steady-state criterion for PhP, which

is fulfilled if

$$\overline{\rho_{\text{PhP},n_0}}^{n_1} \leq \overline{r_{\text{PhP},n_0}}^{n_1} \quad (13)$$

Likewise, for PhH, we obtain

$$\overline{\rho_{\text{PhH},n_0}}^{n_1} \leq \overline{r_{\text{PhH},n_0}}^{n_1} \quad (14)$$

If the conditions imposed by eqs 5, 6, 13, and 14 were met by several data sets, then the set with the biggest number of data points *N* (*N* = *n*₁ - *n*₀ + 1) was used. *N* was required to be at least 10% of the total number of data points in the reduced data set. If this was less than 3, *N* was set to 3.

The steady-state concentrations of PhP and PhH were thus defined by

$$[\text{PhP}]_{\text{sts}} = \overline{[\text{PhP}]}_{n_0}^{n_1} \quad (15)$$

$$[\text{PhH}]_{\text{sts}} = \overline{[\text{PhH}]}_{n_0}^{n_1} \quad (16)$$

and their errors by

$$\sigma_{\text{PhP}} = \rho_{\text{PhP}}[\text{PhP}]_{\text{sts}} + \alpha_{\text{PhP}} \quad (17)$$

$$\sigma_{\text{PhH}} = \rho_{\text{PhH}}[\text{PhH}]_{\text{sts}} + \alpha_{\text{PhH}} \quad (18)$$

where α_{PhP} and α_{PhH} are defined by eqs 3 and 4, respectively, and ρ_{PhP} and ρ_{PhH} are defined by

$$\rho_{\text{PhP}} = \overline{\rho_{\text{PhP},n_0}}^{n_1} \quad (19)$$

$$\rho_{\text{PhH}} = \overline{\rho_{\text{PhH},n_0}}^{n_1} \quad (20)$$

For series 6 and 7, steady-state pH was calculated from the data in the steady-state range determined by the algorithm outlined above. Since the pH was not used as a dependent variable in SteadyFit, no condition with respect to pH was included in the steady-state determination algorithm.

3. Results and Modeling

3.1. Batch Experiments. Titration of TiO₂. Surfaces of metal oxides are generally covered with hydroxyl groups (16). Adsorption of H⁺ and OH⁻ on hydroxylated surfaces can be attributed to protonation and deprotonation of these surface hydroxyl groups (16). For TiO₂, they can be represented by ≡TiOH, where ≡Ti denotes a surface metal center. The titration data were described assuming the mass-action eqs 29, 36, and 37 (Table 3). The surface species ≡TiOH, ≡TiOH₂⁺, and ≡TiO⁻ and the solution species H⁺ and OH⁻ were used in all models describing systems with suspended TiO₂. The equilibrium constants for the formation of ≡TiOH₂⁺ (*K*₈, Table 3) and ≡TiO⁻ (*K*₇) were optimized by fitting calculated total concentration of protons as a function of pH against experimental values. The capacitance value was optimized concurrently and yielded 1.719 Fm⁻². Using the specific surface area obtained from BET measurements (41.67 m² g⁻¹) and the assumption that there were 2.31 sites nm⁻² (17), we calculated a surface site density of 1.60 × 10⁻⁴ mol g⁻¹. Experimental data and fitted curve are shown in Figure 3A.

Adsorption Curves. Adsorption of picolinic acid was modeled using the mass-action eqs 29–31, 36, 37, 40, and 41 (Table 3). Experimental data and fitted curve are shown in Figure 3B, adsorption constants for the surface species ≡TiP (*K*₁₁) and ≡TiOH–P⁻ (*K*₁₂) are given in Table 3. Ludwig (13) reported a similar adsorption behaviour of picolinic acid on TiO₂ supplied by Bayer (Germany). Phenol adsorbed between 20 and 30% (Figure 3C). The adsorption constant for the surface complex ≡TiOH–PhH (*K*₉, eq 38) was optimized using all experimental values obtained after 1–3 days. The surface

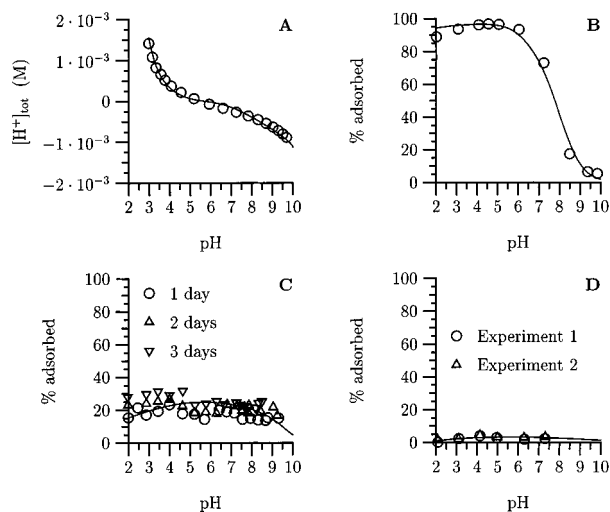


FIGURE 3. Experimental data (symbols) and fitted curves (lines) for acid–base titration of TiO_2 ($\approx 10 \text{ g L}^{-1}$, $[\text{H}^+]_{\text{tot}}$ is the analytical total concentration of H^+ , panel A), adsorption of picolinic acid ($1.0 \times 10^{-4} \text{ M}$, $10.100 \text{ g L}^{-1} \text{ TiO}_2$, panel B), phenol ($1.022 \times 10^{-5} \text{ M}$, $10.583 \text{ g L}^{-1} \text{ TiO}_2$, panel C), and 2-benzoylpyridine ($1.5 \times 10^{-4} \text{ M}$, $9.967 \text{ g L}^{-1} \text{ TiO}_2$, panel D) on TiO_2 . All experiments were performed at room temperature and an ionic strength of 0.1. The adsorption curve of phenol was fitted using the concentrations measured after 1, 2, and 3 days. The adsorption curve of 2-benzoylpyridine was fitted using the data from the duplicates (experiments 1 and 2). The equilibrium constants were determined using the program GRFIT (13).

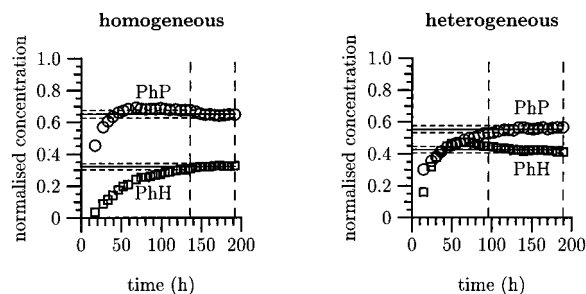


FIGURE 4. Total dissolved concentrations of phenyl picolinate and phenol divided by $[\text{PhP}]_{\text{in}}$ vs time for the homogeneous experiment 3.4 (left) and the heterogeneous experiment 3.1 (right, $12.7 \text{ g L}^{-1} \text{ TiO}_2$). Steady-state pH was 2.55 for both experiments. The concentrations of PhP in the inflow were $8.3 \times 10^{-5} \text{ M}$ and $7.9 \times 10^{-5} \text{ M}$, respectively. The residence time was 20 h for both experiments. The dashed vertical lines delimit the steady-state range. The horizontal lines are the steady-state concentrations (solid) and their error range (dashed).

complexation of 2-benzoylpyridine was modeled analogous to the adsorption of phenol. The equilibrium constants for the protonation (K_{13} , eq 42) and the adsorption (K_{14} , eq 43) reactions of 2-benzoylpyridine were optimized simultaneously. The adsorption was in the range of a few percent, which was also observed by Torrents and Stone (4). Data points and fitted curve are shown in Figure 3D.

3.2. Mixed Flow Experiments. The experimental conditions for the homogeneous and heterogeneous systems are listed in Tables 1 and 2, respectively. In Figure 4, the total dissolved concentrations of phenol, $[\text{PhH}]_{\text{dis}}$, and phenyl picolinate, $[\text{PhP}]_{\text{dis}}$, are plotted versus time for a homogeneous experiment (3.4, left) and a heterogeneous experiment (3.1, right). The steady-state pH was 2.55 in both experiments. The presence of TiO_2 increased the rate of the hydrolysis substantially. The steady-state ranges of these two experiments, which were determined according to the procedure given in section 2.3, are shown by the two vertical dashed lines that delimit the steady-state range. Only data falling in

this range were used to calculate the steady-state concentrations of PhP and PhH (horizontal solid lines) and their error range, $[\text{PhP}]_{\text{sts}} \pm \sigma_{\text{PhP}}$ and $[\text{PhH}]_{\text{sts}} \pm \sigma_{\text{PhH}}$ (horizontal dashed lines).

3.2.1. Homogeneous System. Of the 20 homogeneous experiments, 14 were accepted by the steady-state criteria defined in section 2.3 and were used in the optimization of the kinetic parameters. The volume-normalized flow v ($v = 1/\tau$) as well as the inflow concentration of protons and PhP ($[\text{H}^+]_{\text{in}}$ and $[\text{PhP}]_{\text{in}}$) were taken as independent variables for SteadyFit (8). The steady-state concentrations of phenyl picolinate and phenol, $[\text{PhP}]_{\text{sts}}$ and $[\text{PhH}]_{\text{sts}}$, and their measurement errors, σ_{PhP} and σ_{PhH} , were used as dependent variables for the optimizations. Note that the steady-state pH (pH_{sts}) was not used as a dependent variable. Table 1 lists the experimental conditions for the homogeneous experiments, i.e., the values of the independent and dependent parameters used as input for SteadyFit.

Assuming the hydrolysis reactions



where PhP and PhPH⁺ are the phenyl picolinate species, PH denotes picolinic acid, and PhH denotes phenol, the rate of the homogeneous hydrolysis of PhP can be described by (4, 18)

$$-\frac{d[\text{PhP}]_{\text{dis}}}{dt} = (k_{A1}[\text{H}^+] + k_N + k_B[\text{OH}^-])[\text{PhP}] + k_{A2}[\text{H}^+][\text{PhPH}^+] \quad (23)$$

where k_{A1} , k_N , and k_B are the rate constants for the acid, neutral, and base-catalyzed hydrolysis of PhP and k_{A2} is the rate constant for the acid-catalyzed hydrolysis of the protonated PhP species, PhPH⁺.

For modeling, the species considered were H^+ , OH^- , PhP, PhPH⁺, Ph⁻, PhH, P⁻, PH, PH₂⁺, H₂CO₃, HCO₃⁻, CO₃²⁻, and the components chosen were H^+ , PhP, PH, PhH, and H₂CO₃ (see Figure 2 for structures and abbreviations of organic species). The equilibrium constants for the formation of the species from the components are given in Table 3. Values for the rate constants k_{A1} ($1.600 \times 10^{-3} \text{ M}^{-1} \text{ s}^{-1}$) and k_N ($5.500 \times 10^{-7} \text{ s}^{-1}$) were taken from Torrents and Stone (4). In Figure 5, experimental and calculated $\log k_{\text{obs}}$ values, where k_{obs} is the observed rate constant, are plotted as a function of pH. The circles correspond to k_{obs} , calculated from the measured PhP concentration ($k_{\text{obs,PhP}}$), and the squares correspond to k_{obs} , calculated from the measured PhH concentrations ($k_{\text{obs,PhH}}$). The k_{obs} values were calculated using

$$k_{\text{obs,PhP}} = \frac{[\text{PhP}]_{\text{in}} - [\text{PhP}]_{\text{dis}}}{[\text{PhP}]_{\text{dis}}\tau} \quad (24)$$

and

$$k_{\text{obs,PhH}} = \frac{[\text{PhH}]_{\text{dis}}}{([\text{PhP}]_{\text{in}} - [\text{PhH}]_{\text{dis}})\tau} \quad (25)$$

The first optimization was performed by assuming complete absence of CO_2 (i.e., without carbonic acid species). In this case, the modeled $\log k_{\text{obs}}$ values were substantially smaller than experimental values above pH 6, meaning that the value of k_B was too small (Figure 5, line A).

Two modeling approaches were considered to account for the effect of CO_2 on solution pH:

In the first approach, a kinetic process was included in the model to account for the diffusion of CO_2 into and out of the experimental system. Diffusion of CO_2 was possible at the

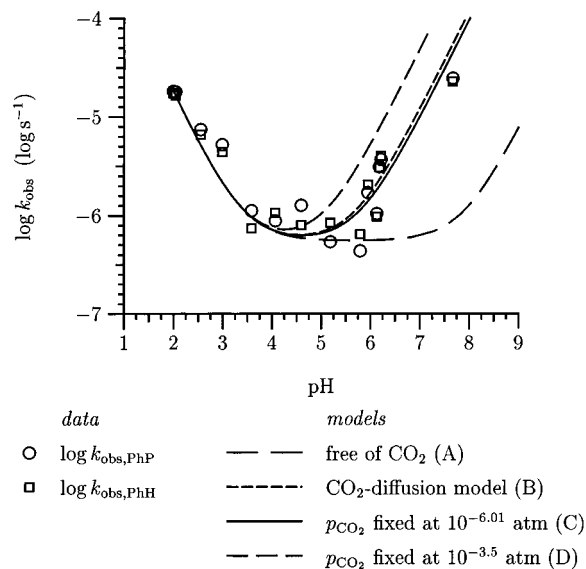


FIGURE 5. Experimental (symbols) and calculated (lines) $\log k_{\text{obs}}$ values for the hydrolysis of phenyl picolinate in homogeneous systems. The lines were calculated using the program SteadyFit. The rate constants for the acid-catalyzed and neutral hydrolysis were taken from Torrents and Stone (4). The other rate constants were optimized using SteadyFit. The curve with $p_{\text{CO}_2} = 10^{-3.5}$ atm corresponds to the case where the aqueous solution in the reservoir is in equilibrium with atmospheric CO_2 . Experiments were performed at 25 °C and an ionic strength of 0.1.

aqueous solution–atmosphere boundary in the aqueous reservoirs but also at the connecting pieces that joined reactors, syringes, and tubing. Some tubes consisted of polytetrafluoroethylene and Tygon (Ismatec tubing), which are not completely impermeable for CO_2 . The rate of the diffusion process, R_{CO_2} , was assumed to be

$$R_{\text{CO}_2} = k_{\text{CO}_2}^{\text{in}} - k_{\text{CO}_2}^{\text{out}} [\text{H}_2\text{CO}_3] \quad (26)$$

The first term, $k_{\text{CO}_2}^{\text{in}}$, defines the rate of CO_2 diffusion into the system and is proportional to the partial pressure of CO_2 in the atmosphere: $k_{\text{CO}_2}^{\text{in}} = k_{\text{CO}_2} p_{\text{CO}_2} K_{\text{H}}$, where K_{H} is Henry's constant ($10^{-1.52} \text{ M atm}^{-1}$, (19)), p_{CO_2} is the partial pressure of CO_2 ($10^{-3.5}$ atm), and k_{CO_2} is the unknown diffusion coefficient of CO_2 of the experimental system. The second term, $k_{\text{CO}_2}^{\text{out}} [\text{H}_2\text{CO}_3]$, describes the diffusion of CO_2 out of the system. Since $k_{\text{CO}_2}^{\text{out}}$ is equal to k_{CO_2} , eq 26 becomes

$$R_{\text{CO}_2} = k_{\text{CO}_2} (p_{\text{CO}_2} K_{\text{H}} - [\text{H}_2\text{CO}_3]) \quad (27)$$

The constant k_{CO_2} was optimized by SteadyFit together with $k_{\text{A}2}$ and k_{B} ($k_{\text{A}2} = 1.982 \times 10^{-3} \pm 0.127 \times 10^{-3} \text{ M}^{-1} \text{ s}^{-1}$, $k_{\text{B}} = 7.008 \times 10^1 \pm 0.690 \times 10^1 \text{ M}^{-1} \text{ s}^{-1}$, $k_{\text{CO}_2} = 1.257 \times 10^{-4} + 0.1424 \times 10^{-4} \text{ s}^{-1}$). The corresponding $\log k_{\text{obs}}$ curve is shown in Figure 5 (line B).

In the second approach, it was assumed that CO_2 entered the system only through the aqueous reservoirs and that purging them with Ar did not remove CO_2 sufficiently. The rest of the experimental system was considered to be closed toward the atmosphere. For each experiment, the total concentration of H_2CO_3 , $[\text{H}_2\text{CO}_3]_{\text{tot}}$, in the reservoir was calculated with MICROQL (20, 21). $[\text{H}_2\text{CO}_3]_{\text{tot}}$ in the reservoir corresponds to the concentration of H_2CO_3 in the inflow of the reactor, $[\text{H}_2\text{CO}_3]_{\text{in}}$. The logarithm of the partial pressure p_{CO_2} was varied in steps of 0.01, and for each p_{CO_2} value, the hydrolysis constants $k_{\text{A}2}$ and k_{B} were optimized with SteadyFit. The partial pressure for which the least-squares function χ^2

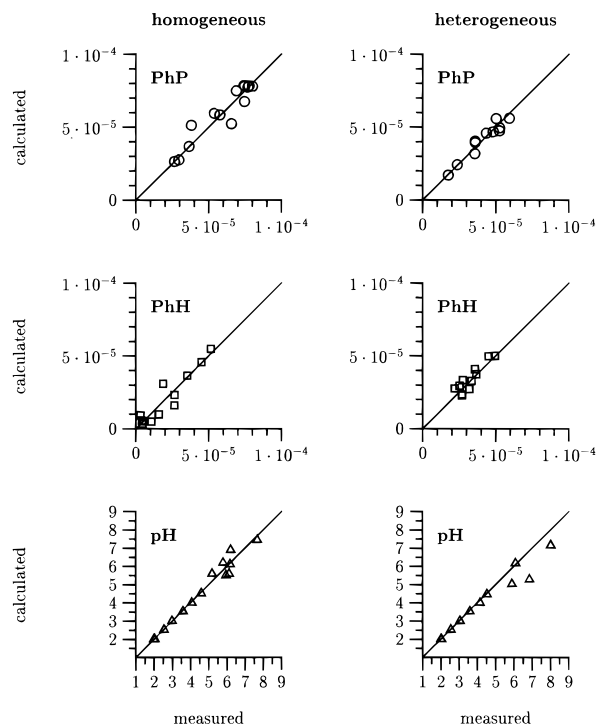


FIGURE 6. Calculated vs measured total dissolved concentrations of phenyl picolinate (PhP), phenol (PhH), and pH. Calculations were performed with SteadyFit after optimization of the homogeneous rate constants $k_{\text{A}2}$ and k_{B} , and the heterogeneous rate constant k_{H} . The partial pressure of CO_2 above the aqueous reservoirs was assumed to be $p_{\text{CO}_2} = 10^{-6.01}$ atm. Concentrations are given in mol L^{-1} .

of the SteadyFit algorithm (eq 3 in ref 8) was minimal was $10^{-6.01}$ atm (Figure 5, line C). The optimized constants were $k_{\text{A}2} = 1.982 \times 10^{-3} \pm 0.127 \times 10^{-3} \text{ M}^{-1} \text{ s}^{-1}$ and $k_{\text{B}} = 57.40 \pm 6.24 \text{ M}^{-1} \text{ s}^{-1}$.

As Figure 5 shows, the $\log k_{\text{obs}}$ curves calculated using the first and the second approach are very close to each other and describe the experimental data much better than the fit without accounting for CO_2 . For comparison, the result of a fit with $p_{\text{CO}_2} = 10^{-3.5}$ is plotted as well (line D). All further calculations were based on the second approach with a fixed CO_2 partial pressure $p_{\text{CO}_2} = 10^{-6.01}$ atm.

The differences between measured and calculated values of $[\text{PhP}]_{\text{dis}}$, $[\text{PhH}]_{\text{dis}}$, and pH for the homogeneous experiments were generally small (Figure 6, left column). The 45° line in Figure 6 was included as eye-guide in each graph and corresponds to equal measured and calculated values. Since pH was not used as a dependent variable in the optimization of the rate constants, the excellent agreement between calculated and measured values indicates that the chosen model gives a consistent description of the experimental system. The deviation between calculated and measured pH values in the pH range 5–7 is due to the experimental uncertainties of pH determination caused by CO_2 and electrode response in this range.

3.2.2. Heterogeneous System. Of the 20 heterogeneous experiments, 13 fulfilled the steady-state criteria, of which 11 were used for the determination of the rate constant for the surface-catalyzed hydrolysis. Experiments 6.1 and 6.2 were discarded because it was uncertain whether steady state was reached. The experimental conditions for the heterogeneous experiments, and hence the input data for SteadyFit, are listed in Table 2.

In the model for the surface-catalyzed hydrolysis, the immobile species $\equiv\text{TiOH}$, $\equiv\text{TiOH}_2^+$, $\equiv\text{TiO}^-$, $\equiv\text{TiP}$, $\equiv\text{TiOH}^-$

P⁻, ≡TiOH-PhH, and ≡TiOH-PhP were added to the species used in the homogeneous model, and the second approach for dealing with CO₂ was used. The additional immobile components are ≡TiOH and EXP, the exponential term used in the constant capacitance surface complexation model. The equilibrium constants of the surface species and the mass-action equations are listed in Table 3. The equilibrium constant *K*₁₀ for the adsorption of phenyl picolinate on the surface of TiO₂ was assumed to be equal to the adsorption constant for 2-benzoylpyridine (*K*₁₄).

The rate of surface-catalyzed hydrolysis can be described by a term proportional to the concentration of the surface complex ≡TiOH-PhP, *k*_H[≡TiOH-PhP] (22). Concentrations of surface species are given in mol L⁻¹. Adding the term *k*_H[≡TiOH-PhP] to eq 23 yields

$$-\frac{d[\text{PhP}]_{\text{dis}}}{dt} = (k_{A1}[\text{H}^+] + k_N + k_B[\text{OH}^-])[\text{PhP}] + k_{A2}[\text{H}^+][\text{PhPH}^+] + k_H[\equiv\text{TiOH-PhP}] \quad (28)$$

for the overall hydrolysis of phenyl picolinate in the heterogeneous system with suspended TiO₂. Formulation of the surface-catalyzed hydrolysis using the term *k*_H[≡TiOH-PhP]-[H⁺] instead of *k*_H[≡TiOH-PhP] did not yield a satisfactory description of the experimental data. In Figure 7, experimental log *k*_{obs} values and calculated log *k*_{obs} curves are plotted as a function of pH. Since the concentration of TiO₂ was generally different for the various experiments (between 7 and 14 g L⁻¹, see Table 2), two log *k*_{obs} curves were calculated: one with 7 g L⁻¹ and the other one with 14 g L⁻¹ TiO₂.

Calculated versus measured values of [PhP]_{dis}, [PhH]_{dis}, and pH are plotted in Figure 6 in the right column. As for the homogeneous experiments, the agreement between calculated and measured values was very good, except for three pH values in the pH 6–9 range.

The model describing the hydrolysis of phenyl picolinate in the presence of suspended TiO₂ particles in mixed flow reactors is defined by the differential eqs 44–48 (Table 4) for the mobile components and by the mass-balance eqs 54 and 55 (Table 5) for the immobile components. After substitution of the total dissolved concentrations (*i*]_{dis}) of each component by eqs 49–53 (Table 5) and replacement of species concentration by the respective mass-action equations (eqs 29–41, Table 3), we obtain the system of differential–algebraic equations needed to calculate the speciation as a function of time. At steady state, the derivatives d*i*]_{dis}/dt are equal to

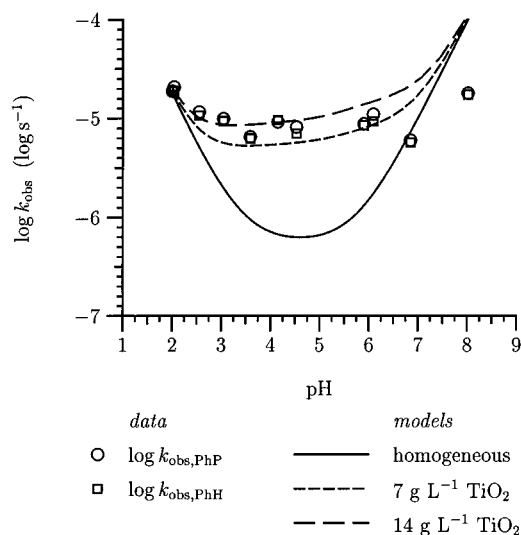


FIGURE 7. Experimental (symbols) and calculated (lines) log *k*_{obs} values for the hydrolysis of phenyl picolinate in heterogeneous systems, and calculated curve for the homogeneous hydrolysis of PhP. Curves have been calculated using Steadyfit after the optimization of rate constant of the surface-catalyzed hydrolysis. Because the concentration of suspended TiO₂ in the experiments was between 7 and 14 g L⁻¹, one curve was calculated for 7 g L⁻¹ and one was calculated for 14 g L⁻¹ TiO₂. The partial pressure of CO₂ above the aqueous reservoirs was assumed to be *p*_{CO₂} = 10^{-6.01} atm. Experiments were performed at 25 °C and an ionic strength of 0.1.

zero, and the system of differential–algebraic equations becomes a system of algebraic equations, which can be solved for the free activity of the components [*i*] by applying a modified Newton–Raphson algorithm (8, 23). For homogeneous systems, the system of equations is reduced by any terms and equations relating to immobile components.

In Figure 8, log *k*_{obs} curves calculated with parameter values determined in this work are compared with curves calculated with parameters taken from the literature. The two curves representing heterogeneous systems in batch and mixed flow reactors were calculated for 10 g L⁻¹ suspended TiO₂. Remarkably, the value of log *k*_{obs} obtained from batch experiments is about 1 order of magnitude higher than the one obtained from the mixed flow experiments. This can be interpreted as the result of a feedback effect caused by the

TABLE 3. Mass-Action Equations and Conditional Stability Constants for Formation of Chemical Species from Components H⁺, PH, PhH, PhP, BP, ≡TiOH, and EXP^a

						log <i>K</i>	
[OH ⁻]	=	<i>K</i> _W	[H ⁺] ⁻¹			-13.78	(29)
[P ⁻]	=	<i>K</i> ₁	[PH]	[H ⁺] ⁻¹		-5.32	(30)
[PH ₂ ⁺]	=	<i>K</i> ₂	[PH]	[H ⁺]		0.77	(31)
[Ph ⁻]	=	<i>K</i> ₃	[PhH]	[H ⁺] ⁻¹		-9.77	(32)
[PhPH ⁺]	=	<i>K</i> ₄	[PhP]	[H ⁺]		1.9	(33)
[HCO ₃ ⁻]	=	<i>K</i> ₅	[H ₂ CO ₃]	[H ⁺] ⁻¹		-6.14	(34)
[CO ₃ ²⁻]	=	<i>K</i> ₆	[H ₂ CO ₃]	[H ⁺] ⁻²		-16.07	(35)
[≡TiO ⁻]	=	<i>K</i> ₇	[≡TiOH]	[H ⁺] ⁻¹		-7.705	(36)
[≡TiOH ₂ ⁺]	=	<i>K</i> ₈	[≡TiOH]	[H ⁺]	[EXP] ⁻¹	3.599	(37)
[≡TiOH-PhH]	=	<i>K</i> ₉	[≡TiOH]	[PhH]	[EXP]	2.299	(38)
[≡TiOH-PhP]	=	<i>K</i> ₁₀	[≡TiOH]	[PhP]		1.350	(39)
[≡TiP]	=	<i>K</i> ₁₁	[≡TiOH]	[PH]		4.337	(40)
[≡TiOH-P ⁻]	=	<i>K</i> ₁₂	[≡TiOH]	[PH]	[H ⁺] ⁻¹ [EXP] ⁻¹	-1.735	(41)
[BPH ⁺]	=	<i>K</i> ₁₃	[BP]	[H ⁺]		1.942	(42)
[≡TiOH-BP]	=	<i>K</i> ₁₄	[≡TiOH]	[BP]		1.350	(43)

^a EXP is the exponential term used in the constant-capacitance model. Values for the stability constants *K*_W, *K*₃, *K*₅, and *K*₆ were taken from ref 25, for *K*₁ and *K*₂ from ref 26, and for *K*₄ from ref 18. Values for *K*₇, *K*₈, *K*₉, *K*₁₁, *K*₁₂, *K*₁₃, and *K*₁₄ were determined using the program GRFIT (73). *K*₁₀ was estimated from 2-benzoylpyridine adsorption experiments (this work).

TABLE 4. Rate of Change of Total Dissolved Concentration (dis) of Each Mobile Component^a

$$\frac{d[H^+]_{dis}}{dt} = v[H^+]_{in} - v[H^+]_{dis} \quad (44)$$

$$\frac{d[PhH]_{dis}}{dt} = -v[PhH]_{dis} + k_{A1}[H^+][PhP] + k_{A2}[H^+][PhPH^+] + k_N[PhP] + k_B[OH^-][PhP] + k_H[≡TiOH-PhP] \quad (45)$$

$$\frac{d[PhP]_{dis}}{dt} = v[PhP]_{in} - v[PhP]_{dis} - k_{A1}[H^+][PhP] - k_{A2}[H^+][PhPH^+] - k_N[PhP] - k_B[OH^-][PhP] - k_H[≡TiOH-PhP] \quad (46)$$

$$\frac{d[PH]_{dis}}{dt} = -v[PH]_{dis} + k_{A1}[H^+][PhP] + k_{A2}[H^+][PhPH^+] + k_N[PhP] + k_B[OH^-][PhP] + k_H[≡TiOH-PhP] \quad (47)$$

$$\frac{d[H_2CO_3]_{dis}}{dt} = v[H_2CO_3]_{in} - v[H_2CO_3]_{dis} \quad (48)$$

^a At steady state, the derivatives are zero, yielding the flux-balance equations for each component.

TABLE 5. Total Dissolved Concentrations of Mobile Components (dis) and Total Concentrations of Immobile Components (tot)^a

$$[H^+]_{dis} = [H^+] - [OH^-] - [P^-] + [PH_2^+] - [Ph^-] + [PhPH^+] - [HCO_3^-] - 2[CO_3^{2-}] \quad (49)$$

$$[PH]_{dis} = [P^-] + [PH] + [PH_2^+] \quad (50)$$

$$[PhP]_{dis} = [PhP] + [PhPH^+] \quad (51)$$

$$[PhH]_{dis} = [Ph^-] + [PhH] \quad (52)$$

$$[H_2CO_3]_{dis} = [H_2CO_3] + [HCO_3^-] + [CO_3^{2-}] \quad (53)$$

$$[≡TiOH]_{tot} = [≡TiOH] + [≡TiOH_2^+] + [≡TiO^-] + [≡TiP] + [≡TiOH-P^-] + [≡TiOH-PhH] + [≡TiOH-PhP] \quad (54)$$

$$[EXP]_{tot} = -[≡TiO^-] + [≡TiOH_2^+] - [≡TiOH-P^-] \quad (55)$$

^a $[≡TiOH]_{tot}$ was a known experimental quantity, and $[EXP]_{tot}$ was calculated assuming the constant-capacitance model (14).

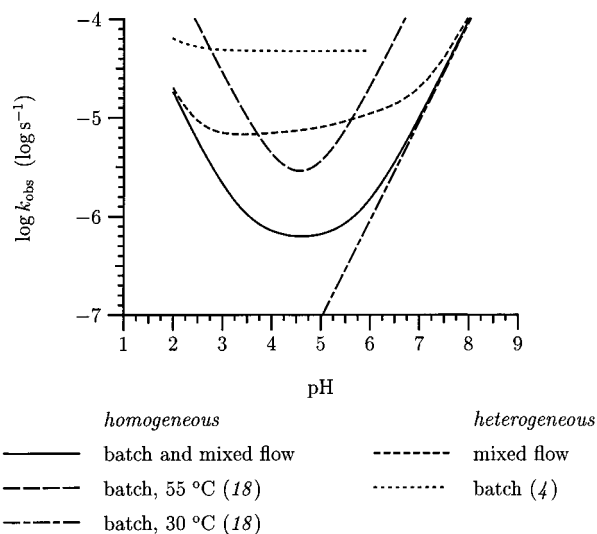


FIGURE 8. Calculated $\log k_{obs}$ curves for the hydrolysis of phenyl picolinate in homogeneous and heterogeneous systems. The temperature was 25 °C except where otherwise noted. The curve for homogeneous hydrolysis at 25 °C was calculated with SteadyFit using the rate constants for acid-catalyzed and neutral reaction published by Torrents and Stone (4) and the rate constants k_{A2} and k_B determined in this work. Homogeneous hydrolysis is assumed to be identical in batch and mixed flow reactors. The partial pressure of CO_2 above the aqueous reservoir solutions was assumed to be $p_{CO_2} = 10^{-6.01}$ atm for the homogeneous as well as the heterogeneous mixed flow system. The curves for the heterogeneous hydrolysis were calculated for $10 \text{ g L}^{-1} TiO_2$. The rate constant for the surface-catalyzed hydrolysis in the batch system was taken from Torrents and Stone (4), and for the mixed flow system, the constant determined in this work was used. Rate constants for the hydrolysis of PhP in homogeneous solutions at 30 °C (base-catalyzed hydrolysis only) and 55 °C were published by Felton and Bruce (18) for an ionic strength of 1.0.

adsorption of products on the surface of TiO_2 , which consequently blocks the reactive sites for the surface-catalyzed hydrolysis of the ester. Obviously, in the presence of TiO_2 , the hydrolytic degradation of PhP is dominated by the surface-

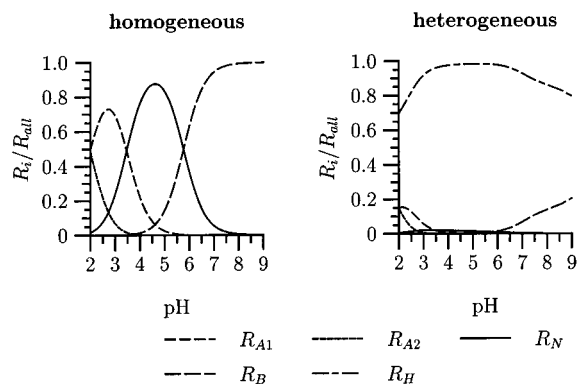


FIGURE 9. Contribution of the individual rates to the overall rate for the hydrolytic degradation of PhP for the homogeneous system (left) and the heterogeneous system (right, $10 \text{ g L}^{-1} TiO_2$) in mixed flow reactors. In the heterogeneous system, the surface-catalyzed hydrolysis is dominant across the whole pH range. The partial pressure of CO_2 is fixed at $10^{-6.01}$ atm. $R_{all} = (k_{A1}[H^+] + k_N + k_B[OH^-])[PhP] + k_{A2}[H^+][PhPH^+] + k_H[≡TiOH-PhP]$, used without the term $k_H[≡TiOH-PhP]$ in the calculation for the homogeneous system. $R_{A1} = k_{A1}[H^+][PhP]$, $R_{A2} = k_{A2}[H^+][PhPH^+]$, $R_N = k_N[PhP]$, $R_B = k_B[OH^-][PhP]$, $R_H = k_H[≡TiOH-PhP]$.

catalytic process (Figure 9). The other two curves have been calculated based on results published by Felton and Bruce (19). They measured the kinetics of the hydrolytic degradation of PhP at an ionic strength of $I = 1.0$ at $T = 30 \text{ °C}$ and at $T = 55 \text{ °C}$. Even though the results cannot be compared directly, they do not appear to be contradictory.

3.2.3. Validation: Calculation of Transient State. The model describing the hydrolytic degradation of PhP in homogeneous and heterogeneous systems was tested by comparing calculated concentration–time series leading to steady state (the transient state) with experimental data. For this purpose, the system of differential–algebraic equations (Tables 4 and 5) was solved for each experiment using the double precision differential–algebraic sensitivity analysis code DDASAC (24). Figure 10 shows the DDASAC results together with measured data for experiments 3.1 and 3.4. The calculated curve of the phenol (PhH) concentration for

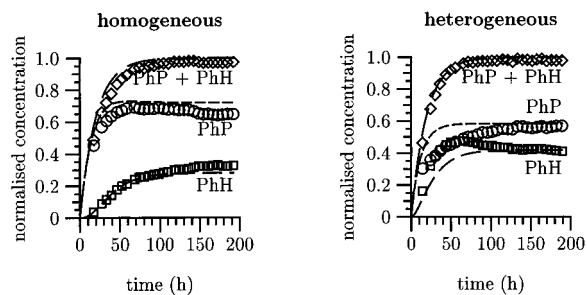


FIGURE 10. Experimental data (symbols) and calculated curves (lines) of the normalized concentrations of phenyl picolinate (PhP) and phenol (PhH) and their sum for experiments 3.4 (left) and 3.1 (right). The lines have been calculated using the double precision differential–algebraic sensitivity analysis code DDASAC (24).

the homogeneous system (experiment 3.4) is in excellent agreement with the measurements, while the calculated concentrations of phenyl picolinate (PhP) at the beginning of the experiment are higher than the measured values. This could be explained by sorption of PhP on the hydrophobic tubing and reactor walls, which may gradually become saturated with the organic compound.

For the initial period of the heterogeneous experiment (experiment 3.1), the agreement between the calculated and observed concentrations of PhP and PhH is not as good as for later times, but the sum of the concentrations is predicted well. It should be noted that the initial concentration of H_2CO_3 , and thus of H^+ , in the reactor as well as the kinetics of the CO_2 outgassing from the reactor are unknown. In general, the agreement between calculated and measured concentrations as well as the sum of the concentrations was satisfactory.

In summary, we can draw the following conclusions. In order to study surface-catalyzed hydrolysis of pesticides in open systems at steady state, an experimental setup using completely mixed flow-through reactors was developed. Steady-state data were analyzed using the computer program SteadyFit (8). The experimental setup and the application of SteadyFit to real experimental data were tested by investigating the hydrolytic degradation of phenyl picolinate and comparing the results with data available in the literature.

The selection of species and components as well as the assumed equilibrium reactions and kinetic reactions and rate laws provided a consistent model for the description of the hydrolytic degradation of phenyl picolinate at steady state. The agreement between predicted and measured concentrations of PhP and PhH in the transient state further indicated that the assumptions were appropriate.

For the homogeneous system, observed rate constants below pH 5 agreed with rate constants calculated using data published by Torrents and Stone (4). For a description of the hydrolysis above pH 5, carbonic acid species had to be included in the model to account for the presence of atmospheric CO_2 in the reaction solutions and its effect on solution pH. Thus, while it is difficult to completely exclude CO_2 from the experimental system, it can be dealt with successfully in chemical models. In the presence of TiO_2 , the rate of hydrolysis was substantially accelerated. In contrast to initial rates obtained from batch experiments, steady-state rates reflected the inhibition of the surface-catalyzed reaction due to co-adsorbed species. This negative feedback effect was also observed in batch reactors by initially adding one of the reaction products, picolinic acid (10).

The fate of organic pollutants in natural systems may be determined by steady-state rates rather than initial rates, depending on the reaction time scale and the residence time of the compounds in the environmental compartment. If

reaction products are involved in reactions influencing the transformation rate of the educt, the steady-state approach presented in this work appears to be the appropriate method for the investigation of chemical kinetics. This method may thus help to understand and predict the long-term fate of pollutants in the environment.

Acknowledgments

Some of the results reported here were obtained by use of GREGPAK, developed at the University of Wisconsin under the supervision of Warren E. Stewart. Helen Schärli performed all batch experiments. We thank Martin Keller, Hanspeter Läser, and Philippe Périsset for their contribution to the experimental setup and René Schwarzenbach and Jörg Klausen for valuable comments. This work was supported by the ETH Research Grant 41–2713.5.

Literature Cited

- (1) Mabey, W.; Mill, T. *J. Phys. Chem. Ref. Data* **1978**, *7*, 383–414.
- (2) Stone, A. T.; Torrents, A. In *Environmental Impact of Soil Component Interactions*; Huang, P., Ed.; Lewis: Chelsea, MI, 1992; pp 275–298.
- (3) Fife, T.; Przystas, T. *J. Am. Chem. Soc.* **1985**, *107*, 1041–1047.
- (4) Torrents, A.; Stone, A. T. *Environ. Sci. Technol.* **1991**, *25*, 143–149.
- (5) Mill, T.; Mabey, W. In *Reactions and Processes*; Hutzinger, O., Ed.; Springer: Berlin, 1988; pp 71–111.
- (6) Furrer, G.; Zysset, M.; Schindler, P. In *Geochemistry of Clay-pore Fluid Interactions*; Manning, D., Hall, P., Hughes, C., Eds.; Chapman & Hall: London, 1993; pp 243–262.
- (7) Levenspiel, O. *Chemical Reaction Engineering*; Wiley: New York, 1972.
- (8) Gfeller, M.; Furrer, G.; Schindler, P. *Geochim. Cosmochim. Acta* **1993**, *57*, 685–695.
- (9) Gfeller, M.; Furrer, G. In *Transport and Reactive Processes in Aquifers*; Proceedings of the IAHR/AIRH Symposium on Transport and reactive processes in aquifers, Zürich, Switzerland, April 11–15, 1994; Dracos, T., Stauffer, F., Eds.; Balkema: Rotterdam, 1994; pp 59–65.
- (10) Torrents, A.; Stone, A. T. *Environ. Sci. Technol.* **1993**, *27*, 1060–1067.
- (11) Torrents, A.; Stone, A. T. *Soil Sci. Soc. Am. J.* **1994**, *58*, 738–745.
- (12) Bald, E. *Chem. Scripta* **1978**, *13*, 47.
- (13) Ludwig, C. Ph.D. Dissertation; University of Berne, Switzerland, 1993.
- (14) Schindler, P.; Stumm, W. In *Aquatic Surface Chemistry*; Stumm, W., Ed.; Wiley: New York, 1987; pp 83–110.
- (15) Furrer, G.; Klausen, J.; Gfeller, M. *Environ. Sci. Technol.* Submitted for publication.
- (16) Schindler, P. In *Adsorption of Inorganics at Solid-Liquid Interfaces*; Anderson, M. A., Rubin, A. J., Eds.; Ann Arbor Science: Ann Arbor, MI, 1981; pp 1–50.
- (17) Davis, J.; Kent, D. In *Mineral-water interface geochemistry*; Hochella, M. F., White, A. F., Eds.; Reviews in Mineralogy Vol. 23; Mineralogical Society of America: Washington, DC, 1990; pp 177–260.
- (18) Felton, S.; Bruice, T. *J. Am. Chem. Soc.* **1969**, *91*, 6721–6732.
- (19) Smith, R.; Martell, A. *Critical Stability Constants. Volume 6: Second Supplement*; Plenum: New York, 1989.
- (20) Westall, J. C. *MICROQL–II. Computation of Adsorption Equilibria in BASIC*; Technical Report; Swiss Federal Institute for Environmental Science and Technology: Dübendorf, Switzerland, 1979.
- (21) Westall, J. C. *MICROQL–I. A Chemical Equilibrium Program in BASIC, Version 2 for PC's*; Technical Report 86–02; Oregon State University: Corvallis, OR, 1986.
- (22) Furrer, G.; Stumm, W. *Geochim. Cosmochim. Acta* **1986**, *50*, 1847–1860.

- (23) Furrer, G.; Westall, J.; Sollins, P. *Geochim. Cosmochim. Acta* **1989**, *53*, 595–601.
- (24) Caracotsios, M.; Stewart, W. *Comput. Chem. Eng.* **1985**, *9*, 359–365.
- (25) Smith, R.; Martell, A. *Critical Stability Constants. Volume 4: Inorganic Complexes*; Plenum: New York, 1976.
- (26) Green, R.; Tong, H. *J. Am. Chem. Soc.* **1956**, *78*, 4896–4900.

Received for review May 21, 1997. Revised manuscript received August 29, 1997. Accepted August 30, 1997.®

ES970440Z

® Abstract published in *Advance ACS Abstracts*, October 15, 1997.